Structural Changes of Escherichia coli Ferric Uptake Regulator during Metal-dependent Dimerization and Activation Explored by NMR and X-ray Crystallography

Ludovic Pecqueur, Benoit d'Autreaux, Jérôme Dupuy, Yvain Nicolet, Lilian Jacquamet, Bernhard Brutscher, Isabelle Michaud-Soret, Beate Bersch

THE JOURNAL OF BIOLOGICAL CHEMISTRY VOL. 281, NO. 30, pp. 21286–21295, July 28, 2006

Structural Changes of *Escherichia coli* Ferric Uptake Regulator during Metal-dependent Dimerization and Activation Explored by NMR and X-ray Crystallography*[S]

Received for publication, February 9, 2006, and in revised form, April 21, 2006 Published, JBC Papers in Press, May 11, 2006, DOI 10.1074/jbc.M601278200

Ludovic Pecqueur[‡§], Benoît D'Autréaux[‡], Jérome Dupuy[¶], Yvain Nicolet[¶], Lilian Jacquamet[¶], Bernhard Brutscher[§], Isabelle Michaud-Soret[‡1], and Beate Bersch[§2]

From the [§]Laboratoire de Résonance Magnétique Nucléaire des Protéines and [¶]Laboratoire de Cristallographie et de Cristallogénèse des Protéines, Institut de Biologie Structurale Jean-Pierre Ebel (Unité Mixte de Recherche 5075 CNRS/Commissariat à l'Energie Atomique/Université Joseph Fourier), F-38027 Grenoble Cedex 1 and [‡]Laboratoire de Physicochimie des Métaux en Biologie (Unité Mixte de Recherche 5155 CNRS/Commissariat à l'Energie Atomique/Université Joseph Fourier), Département Réponse et Dynamique Cellulaires, Commissariat à l'Energie Atomique-Grenoble, 17 Avenue des Martyrs, F-38054 Grenoble Cedex 9, France

Ferric uptake regulator (Fur) is a global bacterial regulator that uses iron as a cofactor to bind to specific DNA sequences. *Escherichia coli* Fur is usually isolated as a homodimer with two metal sites per subunit. Metal binding to the iron site induces protein activation; however the exact role of the structural zinc site is still unknown. Structural studies of three different forms of the *Escherichia coli* Fur protein (nonactivated dimer, monomer, and truncated Fur-(1–82)) were performed. Dimerization of the oxidized monomer was followed by NMR in the presence of a reductant (dithiothreitol) and Zn(II). Reduction of the disulfide bridges causes only local structure variations, whereas zinc addition to reduced Fur induces protein dimerization. This demonstrates for the first time the essential role of zinc in the stabilization of the quaternary structure. The secondary structures of the mono- and dimeric forms are almost conserved in the N-terminal DNA-binding domain, except for the first helix, which is not present in the nonactivated dimer. In contrast, the C-terminal dimerization domain is well structured in the dimer but appears flexible in the monomer. This is also confirmed by heteronuclear Overhauser effect data. The crystal structure at 1.8 Å resolution of a truncated protein (Fur-(1–82)) is described and found to be identical to the N-terminal domain in the monomeric and in the metal-activated state. Altogether, these data allow us to propose an activation mechanism for *E. coli* Fur involving the folding/unfolding of the N-terminal helix.

Iron is an essential element for almost all living organisms. However, the Fe(III) form is highly insoluble, and an excess of Fe(II) is toxic for the cell because of the formation of highly reactive radicals via the Fenton reaction. This is why the intracellular iron concentration has to be tightly regulated. In Gram-negative bacteria, the ferric uptake regulator (Fur)[3] protein plays the key role in regulating iron homeostasis. *Escherichia coli* Fur is a global transcriptional regulator that controls the expression of more than 90 genes mainly implicated in iron uptake but also in other fundamental processes, such as the regulation of oxidative stress, acid tolerance, and bacterial virulence determinants (1).

E. coli Fur is mainly described as a dimeric protein containing two metal-binding sites per subunit. Binding of a divalent cation (ferrous iron *in vivo*) to the regulatory site enables the protein to bind to a specific DNA sequence in the promoter region of iron-regulated genes, the Fur box (2), thus repressing gene transcription. In the regulatory site, the ferrous iron can be replaced by other divalent metal ions, such as Mn(II), Co(II), Zn(II), and Ni(II) (2–4). Previous spectroscopic data (EPR, Mössbauer, and x-ray absorption) indicated that this site forms an axially distorted octahedral environment (5, 6). A second metal site was identified in the 1990s in the *E. coli* Fur protein, which binds Zn(II) with a very high affinity (7, 8). Extended x-ray absorption fine structure studies showed that this zinc ion is coordinated by two cysteines together with one carboxylate and one histidine or two carboxylates (7). The two cysteines, Cys^{92} and Cys^{95}, have been identified as ligands of the zinc atom using chemical modification and mass spectrometry (9). This confirmed the importance of these two cysteines that have been shown to be essential to the *E. coli* Fur activity by site-directed mutagenesis (10). These cysteines are conserved in a large number of Fur proteins, but only one is conserved in *Pseudomonas aeruginosa* Fur. Although the zinc site probably plays a struc-

* The costs of publication of this article were defrayed in part by the payment of page charges. This article must therefore be hereby marked "*advertisement*" in accordance with 18 U.S.C. Section 1734 solely to indicate this fact.
The atomic coordinates and structure factors (code 2FU4) have been deposited in the Protein Data Bank, Research Collaboratory for Structural Bioinformatics, Rutgers University, New Brunswick, NJ (http://www.rcsb.org/).
[S] The on-line version of this article (available at http://www.jbc.org) contains Fig. S1.

[1] To whom correspondence may be addressed: Laboratoire de Physicochimie des Métaux en Biologie, Département de Réponse et Dynamique Cellulaires, CEA-Grenoble, 17 Ave. des Martyrs, 38054 Grenoble Cedex 9, France. Tel.: 33-4-38-78-99-40; Fax: 33-4-38-78-34-62; E-mail: imichaud@cea.fr.
[2] To whom correspondence may be addressed: Laboratoire de Résonance Magnétique Nucléaire, Institut de Biologie Structurale, 41 Rue Jules Horowitz, 38027 Grenoble Cedex 1, France. Tel.: 33-4-38-78-48-25; Fax: 33-4-38-78-54-94; E-mail: beate.bersch@ibs.fr.

[3] The abbreviations used are: Fur, ferric uptake regulator; EDC, 1-ethyl-3-(3-dimethylaminopropyl) carbidiimide; Zn_5FurD, dimeric Fur protein containing zinc in the structural metal site; HSQC, heteronuclear single quantum spectroscopy; NOE, nuclear Overhauser effect; NOESY, nuclear Overhauser effect spectroscopy; DTT, dithiothreitol; MOPS, 4-morpholinepropanesulfonic acid; TOCSY, total correlation spectroscopy; het-NOE, heteronuclear NOE.

tural role, to date no clear function of this zinc site was elucidated.

The only three-dimensional structure of a Fur protein described to date is the metal-activated form of the *P. aeruginosa* Fur (11). The protein was crystallized in the presence of Zn(II) ions. Four metal ions were observed per monomer, two of them were bound to conserved ligands and were therefore proposed to occupy the two characterized relevant sites. From the metal-site geometry in the presence of zinc and after its substitution by iron in the regulatory site, the regulatory and the structural site could be identified (11). In the regulatory site, the zinc ion is hexacoordinated in an octahedral geometry, with a water molecule occupying one of these positions. The structural zinc-binding site contains a zinc ion in a tetrahedral geometry bound to two glutamic acids (Glu^{80} and Glu^{100}) and two histidines (His^{32} and His^{89}) and is therefore different from the one in *E. coli* Fur. It is noteworthy that the single cysteine residue of *P. aeruginosa* Fur was shown to be dispensable for the *in vivo* activity of *P. aeruginosa* Fur by site-directed mutagenesis (12).

Because most Fur proteins contain the conserved cysteines found to be bound to the structural zinc in the *E. coli* protein, it seems essential to study the structural properties of the biochemically well characterized *E. coli* Fur. In addition, no structural information is available on the nonactivated form of Fur.

Here we describe for the first time the structural properties of the nonactivated dimeric *E. coli* Fur (named Zn_SFurD for dimeric Fur protein containing zinc in the structural metal site) by using NMR spectroscopy. In addition, we also studied the so far uncharacterized monomeric form (13) and its conversion to dimer. Finally, a truncated protein comprising the first 82 amino acids, corresponding to the DNA binding domain, has been characterized by NMR and x-ray crystallography. Comparison of the different Fur forms yields essential information on the structural reorganization of this important *E. coli* global regulator during dimerization and activation processes.

MATERIALS AND METHODS

Protein Sample Preparation—Protein purification was performed at 4 °C and centrifugation at 6 °C.

Native *E. coli* Fur was purified to homogeneity according to the published procedure (14). A higher yield in monomeric Fur can be obtained by increasing the EDTA concentration in the extraction buffer to 100 mM. The different oligomeric states of Fur were separated by gel filtration (Superdex 75 16/60 HR; Amersham Biosciences) in 0.1 M Tris/HCl, 0.1 M KCl, pH 8 (4 °C). 10% v/v glycerol was added before protein concentration and storage. Dimer/monomer fractions were pooled separately and concentrated to a final volume of 1 ml by using an ultrafiltration support (Ultrafree 5K, Millipore). Protein concentrations, consistently expressed in subunit concentration unless indicated otherwise, were determined spectrophotometrically by using an absorption coefficient of 0.4 mg^{-1} ml^{-1} cm^{-1} at 275 nm for one monomer of native Fur (15). The Fur-(1–82) mutant was generated by using the QuikChange site-directed mutagenesis kit from Stratagene with the two synthetic oligonucleotide primers 5′-CCGTATTTGAACTGACA**T**AGCAACATCACCACGATC-3′ and 5′-GATCGTGGTGATGTTGCT**A**TGTCAGTTCAAATACGG-3′ and the methylated plasmid pET30c-FUR containing the wild-type protein (14). The constructs were confirmed by DNA sequencing (Genome Express, France). Freshly transformed BL21(DE3) competent cells were plated on LB (0.1% agar) containing 50 μg/ml kanamycin and were grown at 37 °C. Cells were grown at 37 °C from an overnight culture in 1 liter of LB containing 50 μg/ml kanamycin. Fur-(1–82) expression was induced at $A_{600\,nm}$ = 0.7–0.8 by isopropyl β-D-thiogalactoside at a final concentration of 0.5 mM for 3 h. Cells were harvested at 5000 × *g* for 5 min, and the pellet was suspended in 30 ml of 0.1 M MOPS, pH 8, 0.1 M EDTA, 10% w/v sucrose, 10% glycerol (v/v) containing 10 mg/ml trypsin-chymotrypsin inhibitor, 10 μg/ml phenylmethylsulfonyl fluoride, and 4 μg/ml pepstatin A (all from Sigma). Cells were disrupted by sonication, and the supernatant obtained from centrifugation at 20,000 × *g* for 20 min was treated with 1% w/v streptomycin sulfate (Sigma). The suspension was centrifuged for 30 min at 35,000 × *g*. The first step of protein purification consisted of an ammonium sulfate precipitation to 50% of saturation for 3 h followed by centrifugation for 30 min at 25,000 × *g*, the supernatant was brought to 77% ammonium sulfate saturation, and proteins were precipitated under stirring overnight before centrifugation. The precipitate was redissolved in 5 ml of 0.1 M Tris/HCl, pH 8, containing 10% glycerol (v/v). Homogeneous Fur-(1–82) was obtained after a gel filtration on a Superdex 75 HR 16/60 (Amersham Biosciences) equilibrated with 0.1 M Tris/HCl, pH 8.0, 1 M KCl. Pure protein fractions, as revealed by SDS-PAGE and mass spectrometry, were pooled and concentrated with Ultrafree (5K Millipore). Protein concentration was determined with the BCA assay (Bio-Rad) using a FUR and a bovine serum albumin calibration curve. The yield was 30 mg of pure protein per liter of bacterial culture.

Crystallization Conditions and Structure Determination of the Truncated Fur-(1–82)—Screening of the crystallization conditions was initially performed with a TECAN robot at the Institut of Structural Biology using various commercial screens from Hampton Research and Qiagen. Crystals were obtained at 20 °C in 100 mM sodium acetate, pH 4.6, 30% (v/v) PEG 400 containing 100 mM $CdCl_2$ (classic suite from Qiagen). Crystallization conditions were then optimized, and finally, crystals were grown at 20 °C from a 1:1 μl mixture of 10 mg/ml protein solution with 100 mM sodium acetate, pH 4.6, 30% (v/v) PEG 200 containing 100 mM $CdCl_2$. For data collection, the crystals were transferred into a solution composed of the mother liquor containing 25% glycerol as cryoprotectant. X-ray crystallography was then used to obtain the three-dimensional structure of Fur-(1–82) at high resolution.

The final data set was collected at 1.8 Å resolution on beamline FIP-BM30A at the European Synchrotron Radiation Facility, Grenoble, France (16). Data reduction was performed using the XDS program (17). The space group was $P2_12_12$ (a = 38.50 Å, b = 159.27 Å, c = 28.65 Å) with potentially two molecules per asymmetric unit (solvent content of 48%). The structure was solved by molecular replacement performed with the Phaser program (18) using the model of the first 84 amino acids of the *P. aeruginosa* protein (Protein Data Bank code 1MZB). The first model obtained with Phaser was then introduced in

ARP-WARP (19) with the *E. coli* Fur sequence. ARP_WARP built 139 amino acids over the 164 present in the asymmetric unit, and the remaining amino acids have been incorporated with the coot program (20). Refinements of the different models were carried out with the Refmac5 program of the CCP4 Suite (21) in the 30–1.8 Å resolution range without any NCS restraints. The atomic coordinates and structure factors for N-terminal domain of Fur have been deposited with the Brookhaven Protein Data Bank under the accession number 2FU4.

NMR Sample Preparation—Uniformly labeled $^{13}C/^{2}H/^{15}N$- and $^{13}C/^{15}N$/-Fur was obtained by overexpression in the *E. coli* strain BL21(DE3). Bacteria freshly transformed with pET-30-Fur were grown at 37 °C in M9 minimal medium containing 1 g/liter $^{15}NH_4Cl$ and 2 g/liter [^{13}C]glucose with or without ≈95% D_2O and supplemented with $MnCl_2$ (0.1 mM), $ZnSO_4$ (0.05 mM), $FeCl_3$ (0.05 mM), and a vitamin solution (22). ^{15}N-Fur-(1–82) was obtained using the same procedure with minimal medium containing $^{15}NH_4Cl$.

For deuterated Fur, 20 ml of LB medium prepared with 50% D_2O were inoculated with a colony of freshly transformed bacteria, and cells were grown at 37 °C to saturation overnight. Bacteria were harvested at 1500 × *g*, washed twice with 20 ml of cold M9 medium, and resuspended in a final volume of 100 ml of $^{13}C/^{15}N$-labeled M9 medium prepared with ≈95% D_2O. Growth occurred overnight at 37 °C. Cells were harvested at 1500 × *g* and resuspended in 1 liter of $^{13}C/^{15}N$-labeled M9 medium in ≈95% D_2O. The culture was incubated at 37 °C. Expression of the Fur protein was induced with 0.5 mM isopropyl β-D-thiogalactoside when the $A_{600\ nm}$ reached a value of 0.5. Cells were kept at 37 °C for 5 h and were finally harvested and stored frozen at −80 °C until protein purification.

An additional NMR sample of highly deuterated Fur was also prepared using a commercial triple-labeled medium (OD2 medium from Silantes, Germany). After two 10-ml precultures in LB medium prepared with 100% D_2O, 40 ml of triple-labeled OD2 medium were inoculated with 400 μl of cell suspension and incubated overnight at 37 °C. Cells were harvested at 1500 × *g* and resuspended in 920 ml of Silantes OD2 medium. Protein expression was induced by isopropyl β-D-thiogalactoside (final concentration of 0.5 mM) at 37 °C at an $A_{600\ nm}$ of 0.8 for 5 h before harvesting the cells.

For the NMR experiments, the buffer was exchanged to 0.1 M MOPS/NaOH, 0.5 M KCl, pH 7.5, using NAP10 columns (Amersham Biosciences). 7% D_2O and either DTT (10 mM, Fur dimer) or EDTA (20 mM, Fur monomer) were added to the sample after the buffer exchange step.

The high KCl concentration employed was necessary to prevent protein oligomerization at high concentrations.[4] NMR sample concentrations varied between 1.5 and 2.5 mM. All NMR samples were prepared in a glove box under argon and sealed in the NMR tubes.

NMR Spectroscopy—All NMR experiments were performed at 298 K on VARIAN INOVA 600 and 800 spectrometers equipped with triple resonance (^{13}C, ^{1}H, ^{15}N) probes including shielded *z*-gradients. The data were processed using Felix 2000 (Accelrys), and the resonance assignment was achieved using the ALPS program (24). HNCO, HN(CA)CO, HN(COCA)CB, and HN(CA)CB pulse sequences were provided by the Varian protein pack. The three-dimensional MQ-HNCOCA (25) and the three-dimensional MQ-COHNCA (26) were performed as described in the literature. The secondary structure elements were identified from secondary $^{13}C'$ and ^{13}C-α chemical shifts (27). In the case of the dimeric protein, two NOESY experiments were recorded at 600 MHz to deduce the topology of the β-strands as follows: a ^{15}N-edited NOESY-HSQC with a mixing time of 140 ms, and a ^{15}N-HSQC-NOE-^{15}N-HSQC with a mixing time of 50 ms. Both experiments were performed on the highly deuterated Fur sample. For the side chain assignment of the dimeric protein, (H)C(CO)NH-TOCSY and H(CCO)NH-TOCSY experiments were acquired at 600 MHz as well as (H)CCH-TOCSY and H(C)CH-TOCSY experiments at 800 MHz (pulse sequences provided by the Varian Protein Pack). {^{1}H}-^{15}N NOE were measured at 600 MHz using a standard two-dimensional pulse sequence (28). Two spectra with on and off resonance ^{1}H saturation were recorded in an interleaved manner. The saturation time and the recycle delay were set to 4 and 7 s, respectively. Only well resolved peaks were taken into account for the intensity measurements. Resonance assignments for Zn_SFurD and monomeric Fur have been deposited with the BMRB databank under the accession numbers 6947 and 6948, respectively.

Zinc Titration of Monomeric Fur—20 M eq of DTT were added to a solution of 0.8 mM monomeric ^{15}N-labeled Fur in 0.1 M MOPS/NaOH, 0.5 M KCl, pH 7.5. Up to 1.5 M eq/monomer of $ZnSO_4$ dissolved in water was then added drop by drop by steps of 0.5 M eq to the sample in an NMR tube before recording $^{1}H,^{15}N$-HSQC spectra.

RESULTS

E. coli Fur exists in solution under several oligomeric states (29).[4] Monomeric and dimeric species were purified separately because they are not in equilibrium (13, 29).[4] The *E. coli* Fur monomer contains the four cysteines oxidized in two disulfide bridges Cys^{92}-Cys^{95} and Cys^{132}-Cys^{137} (29).[4] Here we describe the structural properties of the dimeric and monomeric forms using NMR and x-ray crystallography, and we investigate the structural changes related to the monomer-dimer conversion.

The $^{1}H,^{15}N$-HSQC spectra of the two forms are shown in Fig. 1. The spectrum of the dimeric protein shows ~150 peaks, from which it can be concluded that Zn_SFurD forms a symmetric dimer, in agreement with the *P. aeruginosa* crystal structure (11). Even if we consider a variation of the chemical environment for residues at the dimer interface, the spectra obtained for the monomer and the dimer are too different for the two species to expect the same three-dimensional structure. In particular, it can be seen that the spectrum of the monomeric protein is less extended both in the proton and in the nitrogen dimension, indicating a lower degree of structuralization of the monomer compared with the dimer.

However, under our NMR experimental conditions, Fur dimer, prepared in the absence of DTT and without strictly

[4] B. D'Autréaux, L. Pecqueur, R. E. M. Diederix, S. Gonzalez de Peredo, C. Caux-Thang, L. Tabet, B. Bersch, E. Forest, and I. Michaud-Soret, submitted for publication.

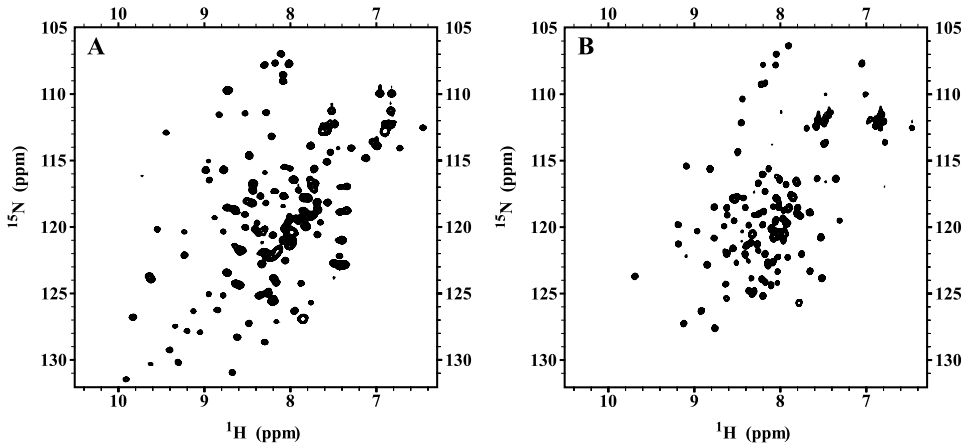

FIGURE 1. **^{1}H, ^{15}N-HSQC spectra of Zn_SFur dimer (*A*) and Fur monomer (*B*).** Both spectra have been acquired at 600 MHz and at a temperature of 25 °C. Sample concentration was 2.0 mM for Zn_SFurD Fur and 1.5 mM for Fur monomer (see "Materials and Methods" for the conditions).

respecting anaerobic conditions, slowly and irreversibly formed some monomeric species. To avoid formation of the monomer, DTT was added to the Fur dimer samples to maintain the cysteines in their reduced form. Furthermore, to avoid formation of oligomeric Fur in the NMR dimer samples, they were prepared in 0.5 M KCl, pH 7.5. The monomeric sample appears stable with time and only shows some proteolytic degradation after several days at room temperature.

NMR Characterization of Nonactivated Fur Dimer (Zn_SFurD)—Using standard three-dimensional NMR experiments, 91% of the backbone resonances could rapidly be assigned. No resonance assignments could be obtained for the five N-terminal residues as well as Val^{67}, Gly^{74}, His^{86}, His^{87}, Asp^{104}, Ser^{105}, and Lys^{116} residues. The secondary chemical shifts derived from the difference between the experimental chemical shift and the one corresponding to a random coil conformation for a specified amino acid indicate the presence of four α-helices (residues 18–24, 35–44, 51–62, and 106–114) and five β-strands (residues 66–71, 77–82, 88–91, 97–102, and 119–131), which are detailed in Fig. 2*A*. The first three helices and the subsequent two β-strands belong to the winged helix-turn-helix motif required for DNA interaction (30). However, the crystal structure of *P. aeruginosa* Fur contains an additional N-terminal helix (11) that we do not observe for the Zn_SFurD protein in solution.

271 and 196 NOEs between amide groups were identified from the ^{15}N-edited NOESY-HSQC and the ^{15}N-HSQC-NOE-^{15}N-HSQC, respectively. This allowed us to deduce the topology of the β-sheets; strands β1 and β2 as well as β3 and β4 form two short antiparallel sheets, and the NOEs observed in the last strand can only be explained by the presence of an antiparallel inter-subunit β-sheet at the dimer interface. These observations are in good accordance with the crystal structure of the Zn(II)-activated *P. aeruginosa* Fur protein (11), with the exception of the N-terminal helix preceding the winged helix-turn-helix motif.

Unfortunately, further structural investigations of the protein by NMR were made impossible by the very unfavorable relaxation properties of this protein. The difficulty of the NMR study of Fur was already described in the literature (31–33). Only about 40% of the side chain resonances could confidently be assigned. Attempts to obtain additional structural information from ^{13}C-edited NOESY spectra failed. ^{15}N relaxation measurements revealed that the ratio of transversal and longitudinal relaxation rates was much higher than expected from the molecular mass of 34 kDa (results not shown), and we suppose that under our experimental conditions there is still some amount of oligomeric protein formed in the sample during data acquisition.

NMR Characterization of Fur Monomer—In case of the monomeric Fur, the backbone resonance assignment could be achieved easily for the N-terminal domain. Four α-helices (residues 5–9, 17–24, 35–44, and 51–63) and two β-strands (residues 67–71 and 76–80) were deduced from the analysis of the secondary chemical shift values (Fig. 2*B*). The C-terminal domain (residues 81–147) was difficult to assign, and 26 residues of 67 could not be identified. Moreover, 16 peaks were missing in the ^{1}H,^{15}N-HSQC, indicating that the monomer probably undergoes conformational exchange. The secondary chemical shifts do not indicate any well defined secondary structure elements in the C-terminal domain, which is known to be involved in the dimer interface.

Compared with Zn_SFurD, the N-terminal domain has globally the same secondary structure except for the first residues, for which the secondary chemical shifts reveal the presence of an additional α-helix (residues 5–9), situated N-terminal to the helix-turn-helix motif, analogous to the one seen in the *P. aeruginosa* protein.

Comparison of Monomeric and Dimeric Species—The comparison of the backbone chemical shifts between monomer and dimer is shown in Fig. 2*E*. It can be seen that there are no deviations or only very weak deviations in the region corresponding to the helix-turn-helix motif (residues 14–65), suggesting that the local structure of this part of the protein is not influenced by the dimerization. On the other hand, there are significant differences for the C-terminal half and for the 18 N-terminal residues, regions for which the analysis of the secondary chemical shift has already indicated very different structural behavior (see Fig. 2, *A* and *B*). To confirm the structural flexibility of the C-terminal domain in the monomeric species and to obtain further information on the intriguing changes in secondary structure in the N-terminal part between mono- and dimer, {^{1}H}-^{15}N heteronuclear NOE (het-NOE) spectra were recorded for both forms. The het-NOE allows us to obtain information on the reorientation of the amide bond on the pico- to nanosecond time scale. Generally, {^{1}H}-^{15}N het-NOE values above 0.7 indicate that the N-H vector is rigid with respect to the rest of the protein, whereas smaller values are due to increased backbone mobility.

In both the dimer and the monomer, residues previously determined to be situated in secondary structure elements are

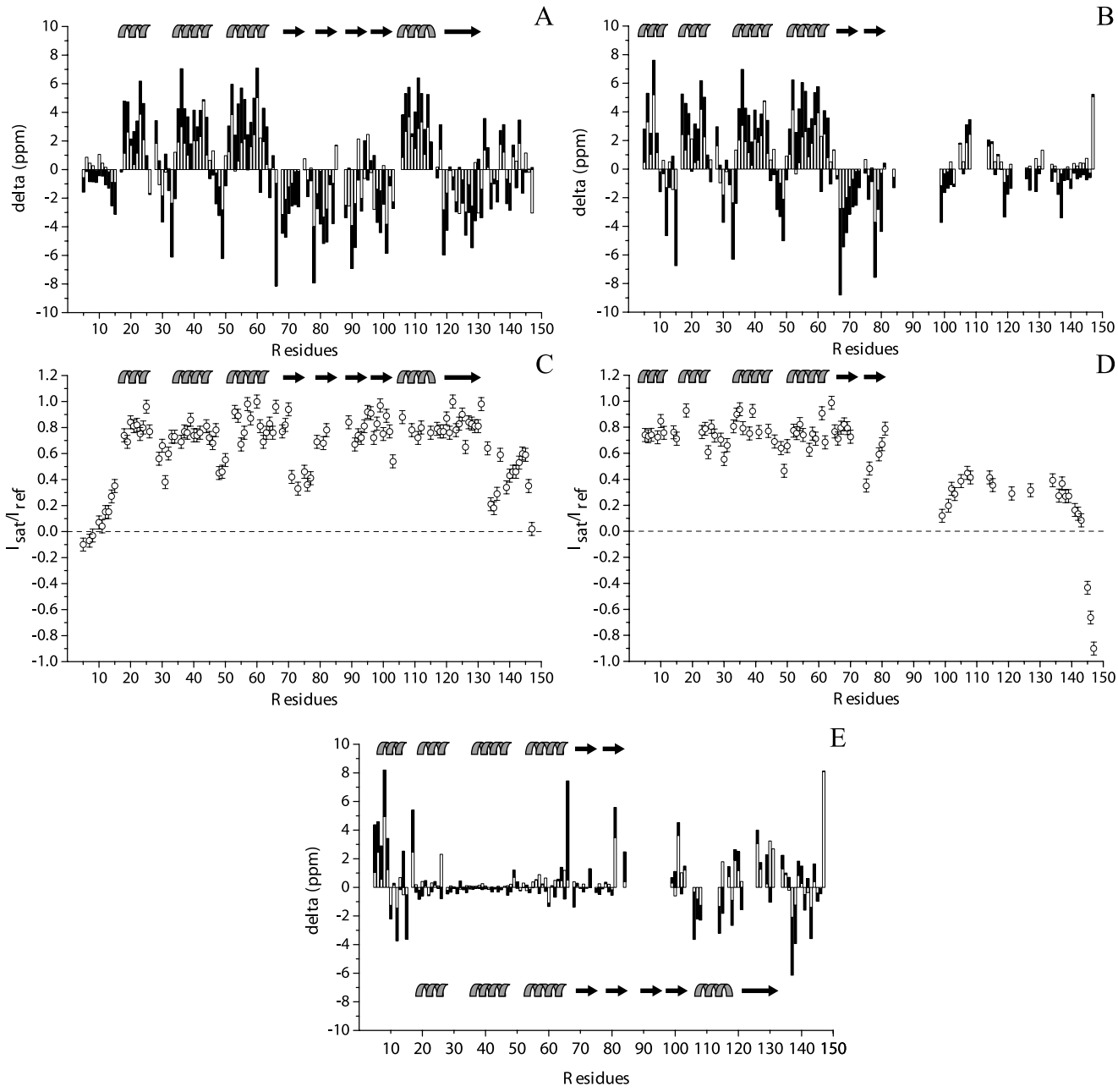

FIGURE 2. **NMR comparison of Zn_5Fur dimer and Fur monomer.** *A* and *B,* secondary structures determined from secondary chemical shift values observed for C′ (*open bars*) and C-α (*filled bars*) in the dimer (*A*) and in the monomer (*B*). *C* and *D,* heteronuclear NOE values determined for Zn_5FurD (*C*) and Fur monomer (*D*) at 600 MHz and 25 °C. *E*, chemical shift difference (FurM-Zn_5FurD) for backbone HN (*white bars*) and N (*black bars*) between the two forms. For each form, the secondary structure elements as determined from chemical shift analysis are given.

characterized by $\{^1H\}$-^{15}N het-NOE values greater than 0.7 (Fig. 2, *C* and *D*). However, even in the more structured dimer, loops connecting the secondary structure elements are found to be quite flexible with $\{^1H\}$-^{15}N het-NOE values below 0.5. In addition, both the N-terminal and the C-terminal residues appear mobile in the dimeric Fur protein. The low $\{^1H\}$-^{15}N het-NOE values measured for the 15 N-terminal residues confirm the absence of the additional N-terminal helix identified in the monomeric protein. So, overall the dimeric nonactivated Fur does not appear as a structurally well ordered protein, which may explain the difficulties in getting crystals for x-ray analyses.

In the monomeric protein, the N-terminal DNA-binding domain appears to be rigid, including residues 6–10, thus confirming the presence of an additional α-helix. On the contrary, the C-terminal domain is characterized by $\{^1H\}$-^{15}N het-NOE values below 0.5, demonstrating its poorly structured nature.

Monomer to Dimer Conversion—In the dimer, the four cysteines are reduced in contrast to the monomer, in which they were found oxidized[4] (data not shown) and involved in disulfide bridges between cysteines Cys^{92} and Cys^{95} on one hand and Cys^{132} and Cys^{137} on the other hand. We found that formation of dimer required reduction of the disulfide bonds and incorporation of Zn(II), but reduction of the four cysteines by DTT alone did not promote dimerization.[4] We further investigated the structural changes following reduction of cysteines and addition of Zn(II) ions using NMR. ^1H,^{15}N-HSQC spectra of

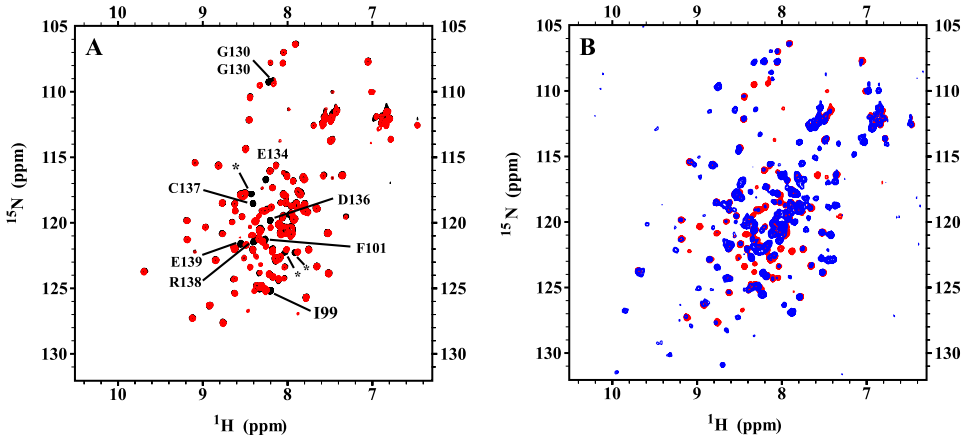

FIGURE 3. **Monitoring reduction and zinc titration of Fur monomer by NMR.** *A*, superposition of the ^{1}H,^{15}N-HSQC spectra of the oxidized (*black*) and reduced monomer (*red*). The annotated peaks correspond to residues that move after the addition of 1 eq of DTT. *B*, addition of zinc to DTT-reduced Fur monomer leads to the appearance of the Zn_5FurD ^{1}H,^{15}N-HSQC spectrum. The correlation peaks of reduced Fur monomer before and after the addition of 0.9 M eq of $ZnSO_4$ are shown in *red* and *blue*, respectively.

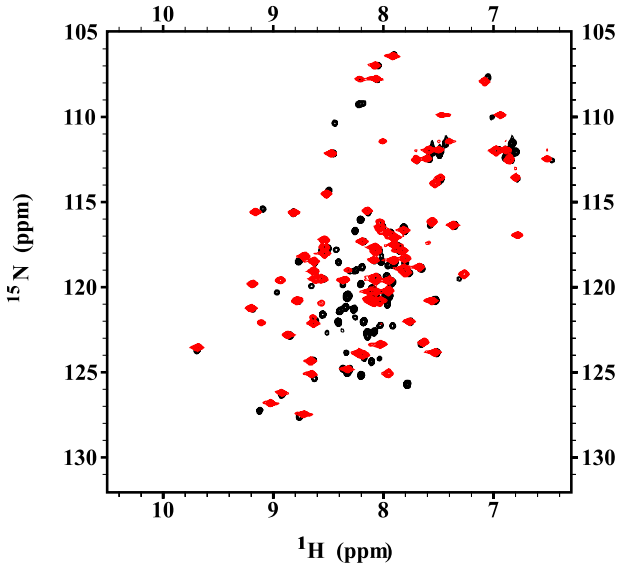

FIGURE 4. **Comparison of the ^{1}H,^{15}N-HSQC spectra of monomeric Fur and truncated Fur-(1–82).** The two spectra are superimposed with the spectrum of monomeric Fur shown in *black* and that of Fur-(1–82) in *red*. The *black* resonance peaks in the center of the spectrum belong to the unstructured C-terminal domain.

the monomer recorded in the absence or presence of DTT are shown in Fig. 3*A*. These spectra indicate that no major structural changes occur upon reduction. Only a few ^{1}H,^{15}N-correlation peaks shift, which are mostly located around the Cys^{132} and Cys^{137}. The addition of Zn(II) to the reduced monomer leads to the appearance of ^{1}H,^{15}N-correlation peaks that belong to the dimer spectrum. Under nonsaturating conditions with zinc, the ^{1}H,^{15}N-HSQC spectra of both forms coexist, indicating that both forms are in slow exchange with respect to the NMR time scale (compare Fig. 3*B*). The spectrum obtained in the presence of 0.95 M eq of Zn(II) still shows the presence of monomeric Fur, probably because of the excess of DTT also chelating competitively the Zn(II) in solution and thus decreasing the amount of metal available for the protein. It was not possible to completely saturate the zinc site of the Fur protein because at higher Zn(II) concentrations precipitation occurred.

We therefore confirm that the incorporation of Zn(II) is essential for a large structural reorganization related to Fur dimerization and that the dimer formed from the reduced monomer is identical to the native dimeric protein.

Structural Characterization of the Truncated Fur, Fur-(1–82)—As more detailed structural studies of the dimeric *E. coli* Fur protein were extremely difficult, we decided to further characterize the monomeric form. A truncated protein formed only by the N-terminal DNA-binding domain was produced as the C-terminal domain has been shown to be disordered in monomeric Fur. ^{15}N-Labeled truncated Fur-(1–82) was obtained and an ^{1}H,^{15}N-HSQC spectrum acquired. Fig. 4 shows the superposition of the ^{1}H,^{15}N-HSQC spectra of monomeric and truncated *E. coli* Fur. These spectra are almost identical, and we can therefore conclude that the structure of the isolated N-terminal domain is only slightly changed with respect to the corresponding fragment of monomeric Fur.

X-ray crystallography was then used to obtain the three-dimensional structure of Fur-(1–82) at 1.8 Å resolution, which is shown in Fig. 5. The final model contains residues 1–82 from each monomer present in the asymmetric unit as well as 180 water molecules. The asymmetric unit includes two monomers with the interaction surface formed by helix 4 and strand 1 and two Cd(II) cations. This interface, involving two cadmium ions, is certainly not biologically relevant as it contains helix 4, the DNA recognition helix. In addition, this dimeric form is incompatible with the native dimeric protein in which the C-terminal domain provides the inter-subunit interface (11). The structure of one subunit is composed of four α-helices (residues 3–10, 16–25, 35–45, and 51–64) and two β-strands forming an antiparallel sheet (66–72 and 76–82), a secondary structure composition identical to the one found in the dimeric and zinc-activated *P. aeruginosa* Fur (11). All residues fall within the allowed regions of the Ramachandran plot as defined by the PROCHECK program (34). Statistics for all the data collections and refinement of the different structures are summarized in Table 1. The structure of truncated *E. coli* Fur-(1–82) can be remarkably well superimposed with the N-terminal domain of the *P. aeruginosa* Fur protein, with a root mean square deviation of 0.8 Å (calculated for 312 backbone atoms). Local variations of the backbone conformation are observed for two loops, the one connecting helix 2 and helix 3 and the turn between the two β-strands (Fig. 5). It should be mentioned that the N-terminal helix of Fur-(1–82) is perfectly superimposed to the one in the *P. aeruginosa* Fur. In the truncated Fur-(1–82), residues from this helix are involved in hydrophobic contacts with Leu^{19}, Leu^{22} on helix 2, Phe^{61}, Ala^{64} on helix 4, as well as Ile^{66} and Leu^{12}, both situated in loop regions. As also observed for the *P. aeruginosa* Fur, positively charged residues situated at the end of the N-terminal helix

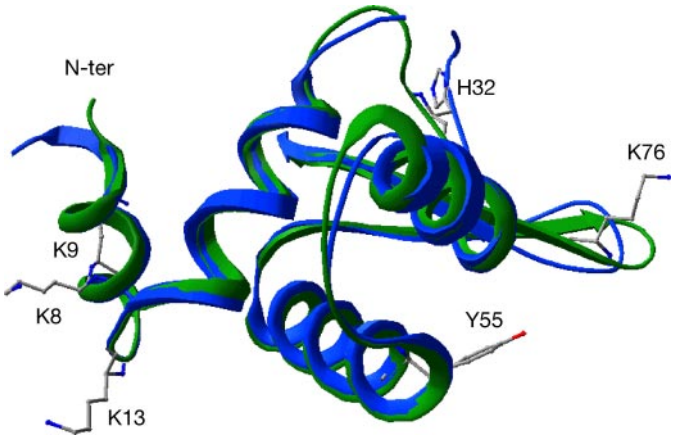

FIGURE 5. **X-ray structure of truncated Fur-(1–82).** *Ribbon* representation of *E. coli* Fur-(1–82) (*green*) superposed on the N-terminal domain of *P. aeruginosa* Fur. The structures have been superimposed using the SwissPdbViewer (44). Several side chains of amino acids discussed in the text and the literature are shown as follows: the Lys[76] and the Tyr[55] side chains proposed to be in interaction with the DNA (23, 30), the His[32] bound to the structural zinc in *P. aeruginosa* Fur and Lys[8], Lys[9], and Lys[13] proposed to be protected from methyl acetamidate reactivity upon DNA binding (30).

(Lys[8], Lys[9], and Lys[13] in *E. coli* Fur) contribute to a basic surface patch that can be assumed to be essential for protein-DNA interaction. Comparison of the electrostatic surfaces of *E. coli* Fur-(1–82) and *P. aeruginosa* Fur is shown in Fig. S1. Again, these surfaces are very similar, indicating a conserved DNA-interaction mechanism.

DISCUSSION

During the last 2 decades, numerous research groups have contributed interesting and complementary results on the structural and functional aspects of Fur proteins, global transcriptional regulators ubiquitous in Gram-negative bacteria. In 2003, the crystal structure of the Fur protein from *P. aeruginosa* was published (11), providing the first detailed structural information of a Fur protein on a molecular level. This structure corresponds to the zinc-activated protein, containing zinc in the two metal-binding sites (structural zinc and regulatory iron sites). However, spectroscopic and biochemical data have shown that at least for the structural zinc site, *P. aeruginosa* and *E. coli* Fur proteins show differences, which might be related to their specific function in the different organisms. The importance of the cysteines is clearly different in *E. coli* and in *P. aeruginosa* Fur because the two of them bound to the zinc in *E. coli* Fur have been shown to be essential to *E. coli* Fur activity by site-directed mutagenesis (10). On the contrary to the single cysteine residue of *P. aeruginosa* Fur that was shown to be dispensable for the *in vivo* activity of *P. aeruginosa* Fur also by site-directed mutagenesis (12).

Therefore, structural information on additional Fur proteins is necessary for a better understanding of the structure-function relationship within the Fur family. In addition, no structural data were available for the nonactivated protein. Biochemical data obtained on the *E. coli* protein have clearly shown that metal binding induces conformational changes (30)[4] related to the activation mechanism. For these reasons, we started to investigate the structural properties of the *E. coli* Fur protein in its nonactivated dimeric form.

TABLE 1
Data collection statistics

Data collection	
Resolution (Å)[a]	50-1.8(1.9-1.8)
Space group	$P2_12_12$
Unit cell parameters	a = 38.5 Å; b = 159.1 Å; c = 28.6 Å
Total no. of reflections	145,937
Total no. of unique reflections	17,195
*R*sym (%)[a,b]	9.2 (32.9)
Completeness (%)[a]	99.4 (97.1)
$I/\sigma(I)$	17.72 (6.19)
Redundancy	8.5
Refinement	
Resolution (Å)	28-1.8
R_{factor} (%)[c]	17.2
R_{free} (%)	21.5
Structure quality	
R.m.s.d.[d] bonds (Å)	0.011
R.m.s.d. angles (°)	1.276

[a] Numbers in parentheses are for highest resolution shell.
[b] $R_{merge} = \Sigma_h\Sigma_i|I_{hi} - \langle I_h\rangle|/\Sigma_h\Sigma_i I_{hi}$, where I_{hi} is the ith observation of the reflection h, and $\langle I_h\rangle$ is the mean intensity of reflection h.
[c] $R_{factor} = \Sigma\,||F_o| - |F_c||/|F_o|$. R_{free} was calculated with a small fraction (5%) of randomly selected reflections.
[d] R.m.s.d. indicates root mean square deviation.

Fig. 6 shows the sequence alignment of *P. aeruginosa* and the *E. coli* Fur together with the experimentally determined secondary structure elements. By comparing the structural information available from the solution study of dimeric, nonactivated *E. coli* Fur with the crystal structure of *P. aeruginosa* Fur, we have shown that the overall architecture is conserved; the size, the localization, and the topology of the secondary structure elements seem to be identical, as far as we can conclude from our NMR data. There is only one remarkable exception: the additional N-terminal helix, which has also been predicted from the *E. coli* Fur protein sequence. This helix is present in the activated *P. aeruginosa* protein, but our results show that it is absent in the nonactivated form of Fur from *E. coli*. We first thought that the presence of this helix in the *P. aeruginosa* crystal structure might be related to an altered N terminus (addition of two residues resulting from the cleavage of the glutathione *S*-transferase fusion protein) or to the crystal environment. However, our observation of an analogous helix in the monomeric form of the *E. coli* Fur protein in solution as well as in the truncated Fur N-terminal domain demonstrates that this region is able to fold as an α-helix also in the *E. coli* protein. We thus became interested in this N-terminal helix and its possible role within the DNA-binding domain.

It has already been suggested by Pohl *et al.* (11) that the N-terminal helix is required for efficient DNA binding. This is further supported by mutagenesis studies; for example, *P. aeruginosa* Fur, having Ala[10] mutated to glycine, a much poorer helix former, was found to be unable to bind to the *pvdS* promoter (35), and in *E. coli* it has been shown that proteolytic cleavage of the 8 or 9 N-terminal residues resulted in a protein with reduced DNA-binding affinity and specificity (36). By comparing the sequences of different Fur proteins it can be seen that in addition to a highly conserved basic residue in the loop connecting the first two helices (Lys[13] in *E. coli*), one or two lysine or arginine residues are often found at the end of the N-terminal helix. These lysine side chains are surface-exposed and could thus be involved in DNA recognition and interaction. One can imagine that folding of the N-terminal residues in an

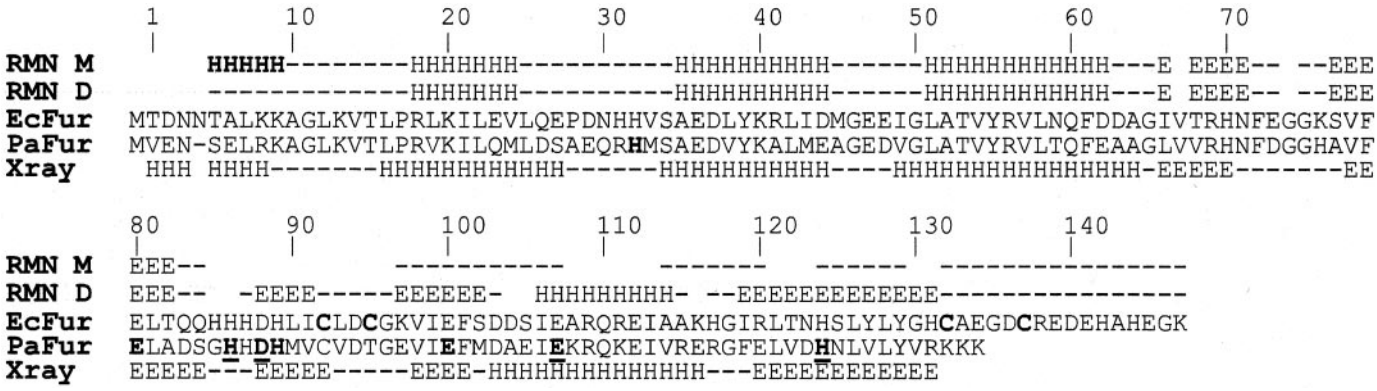

FIGURE 6. **Sequence alignment of Fur from *P. aeruginosa* and *E. coli* and secondary structure comparison.** Metal-binding ligands are in *boldface* in the corresponding sequence as follows: *underlined boldface* for the regulatory iron site and *boldface* for the structural zinc site. Experimentally determined secondary structure elements are indicated with E for β-strands, H for α-helices, and – for unstructured. *Blanks* correspond to unassigned residues in *E. coli* Fur.

α-helical conformation stabilizes these side chains in a position suitable for DNA recognition and interaction.

The absence of this N-terminal helix in the nonactivated protein in solution together with the structural considerations mentioned above suggest that the presence of the N-terminal helix is related to the activation state of the dimeric Fur protein. Metal binding to the functional iron site would induce conformational changes resulting in the stabilization of the N-terminal residues in an α-helical conformation, thus optimizing DNA recognition and interaction. However, looking at the crystal structure of dimeric and activated *P. aeruginosa* Fur protein, it becomes difficult to imagine how the C-terminal regulation domain could communicate with the distant N-terminal helix in the DNA-binding domain. The results we obtained in this study on the three different forms of Fur may provide a clue for a possible activation mechanism of the Fur protein, involving the N-terminal helix. Comparison of the $^{1}H,^{15}N$-HSQC spectra of the three forms indicates that the structure of the winged helix-turn-helix motif (helices 2–4, strands 1 and 2) is independent of the state of the C-terminal domain: folded (Zn_S-FurD), unfolded (Fur monomer), or absent (truncated Fur-(1–82)). The only difference between these forms is the absence or presence of the additional N-terminal helix, which we have identified in the two monomeric forms (Fur monomer and truncated Fur-(1–82)). From this observation we can conclude that it is the sole presence of the structured C-terminal domain in the dimeric nonactivated protein, which triggers the unfolding of the N-terminal helix. The unfolded state of the corresponding residues has experimentally been demonstrated by the NMR relaxation measurements (compare Fig. 2*D*). Furthermore, EDC cross-linking experiments have shown the spatial proximity of the N-terminal amino group of one subunit and a carboxyl group within the C-terminal last 9 residues of the second (37).[4] In addition, experiments using a dimethyl adipimidate cross-linker demonstrated intersubunit contacts between the N-terminal extremity of one subunit and Lys^{76} and Lys^{97} (37).[4] These contacts are not compatible with the crystal structure of activated *P. aeruginosa* Fur with an α-helical N terminus (see Fig. 7) but could be explained by a more elongated and flexible conformation of the N-terminal residues. Metal binding to the C-terminal activation site abolishes effective intersubunit cross-links involving EDC as well as dimethyl adipimidate (37),[4] providing additional experimental evidence for the reorganization of the N-terminal residues. We therefore suggest that the activation of *E. coli* Fur proceeds by metal binding to the C-terminal domain that triggers local conformational changes. This then unlocks the experimentally observed interactions with residues in the unstructured N-terminal part, leading to formation of helix 1 and thus of the DNA recognition site involving the basic residues directly adjacent to this helix. This mechanism may involve a relative reorientation of the two subunits, which could contribute to the decrease of the distance between the N terminus and parts of the other subunit.

To clarify this issue, additional structural studies of the nonactivated form of the Fur protein are necessary. A structural characterization at high resolution of this form would help to gain insight into the global structural reorganization leading to such a drastic change in secondary structure because of the binding of the activating metal ion.

It should be mentioned that the presence of this additional N-terminal helix is very untypical for transcriptional regulators with a winged helix-turn-helix motif. Proteins of the MarR family like MarR (38) or MexR (39) have been shown to possess an extra N-terminal helix, but in these two proteins this helix is involved in dimerization by directly interacting with the C-terminal dimerization domain. To our knowledge, the implication of such an N-terminal helix in DNA recognition and the regulation of DNA binding activity have never been reported in the literature and might be a unique feature of the Fur proteins.

Besides the switch from the nonactivated to the metal-activated form, *E. coli* Fur also undergoes a metal-induced, redox-controlled monomer-dimer transition that depends on Zn(II) binding to the structural metal site. By using NMR spectroscopy, we show that the monomer is characterized by an unstructured C-terminal dimerization domain and that addition of Zn(II) to the reduced monomer leads to the regeneration of Zn_SFurD. Therefore, zinc binding induces structural changes that enable the structuralization of the C-terminal domain and dimerization.

In *E. coli* Fur, the structural zinc is bound by two cysteine residues, as formerly shown by extended x-ray absorption fine structure spectroscopy (7). They were identified and correspond to Cys^{92} and Cys^{95} (9). One of these two cysteines is missing from the *P. aeruginosa* Fur protein, and the

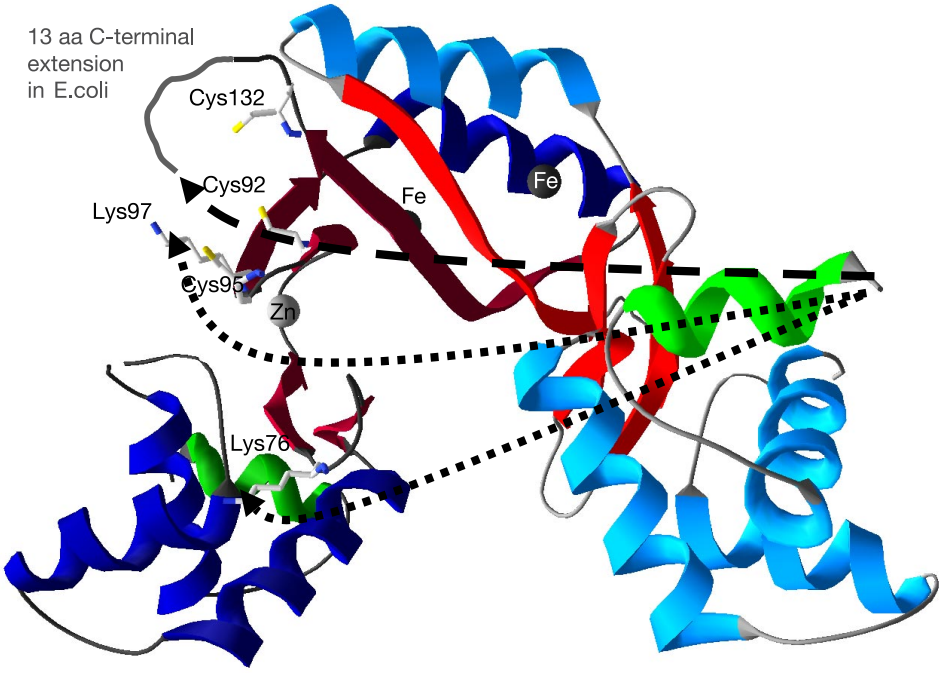

FIGURE 7. **Structural model of activated *E. coli* Fur.** The two different subunits are shown in different *blue tones*; the N-terminal α-helices are indicated in *green* and the β-strands in *red*. The two zinc atoms present in each subunit of *P. aeruginosa* Fur structure are shown, and the Cys^{92} and Cys^{95} residues that have been shown to participate in the structural zinc site in *E. coli* Fur are represented in detail. The localization of the Cys^{92}, Cys^{95}, and Cys^{132} side chains are deduced from a homology model of *E. coli* Fur created with SwissModel (44) from the *P. aeruginosa* Fur structure, in which only Cys^{92} is conserved. The experimentally observed cross-links with dimethyl adipimidate and EDC are indicated by the *dotted* and *dashed arrows,* respectively. Side chains involved in intersubunit cross-links obtained on the nonactivated Fur are displayed.

crystal structure reveals that zinc is tetra-coordinated by four conserved amino acids. two histidines and two glutamic acids. In *P. aeruginosa* Fur, the zinc ligands are located both in the N- and in the C-terminal domain, holding together the two antiparallel β-sheets. In a homology-based structural model of *E. coli* Fur, Cys^{92} and Cys^{95} are situated in the loop connecting the two strands of the second antiparallel β-sheet and are far from the zinc-binding site in *P. aeruginosa* Fur (Fig. 7). Thus, the zinc-binding site is clearly different from the one in *E. coli* Fur and may not be strictly conserved among the Fur proteins.

This observation is also confirmed by recent results obtained on the Fur protein from *Bradorhizobium japonicum*. By using atomic absorption spectroscopy, the authors showed that *Br. japonicum* Fur does not contain a structural zinc ion, although they were able to correctly demonstrate the presence of zinc in *E. coli* Fur (40). In addition, they performed mutagenesis studies in which the residues corresponding to either of the two metal-binding sites identified in the crystal structure have been mutated. These mutants still bind DNA with high affinity and repress transcription in an iron-dependent manner (39), which led the authors to suggest that the Fur protein might be a structurally and functionally more diverse protein than previously supposed.

Looking at the sequence alignment of the Fur family (41), it can be realized that most of the Fur proteins in which the two cysteine residues corresponding to Cys^{92} and Cys^{95} in *E. coli* are conserved also contain a second pair of cysteines in a C-terminal extension. The first of these two additional cysteines (Cys^{132}) could be modeled in the three-dimensional structure for *E. coli* Fur and is separated by less than 8 Å from Cys^{92} and Cys^{95} (Fig. 7). From our results in *E. coli* Fur, we know that this cysteine 132 is not implicated in zinc binding (9) and is not essential for the *in vivo* activity (10). However, in Fur-like proteins functioning as oxidative stress sensors, like FurS or PerR, the cysteine homologous to Cys^{132} in *E. coli* is found in a CX_2C motif in contrast to the CX_4C motif encountered in *E. coli* Fur. A very recent structural model based on mutagenesis studies was proposed for PerR of *Bacillus subtilis* (42), in which the zinc was bound by these four cysteines.

All these data provide evidence that the zinc site is not strictly conserved among the Fur and Fur-like proteins and may have evolved in function of the specific requirements in the whole regulation network of a given bacterial strain. For instance, zinc bound to sulfur ligands can be involved in redox regulation of important protein functions (43).

The present NMR studies of the monomeric protein confirm the importance of the zinc site for the structural integrity of the dimeric protein. We can hypothesize that this observed redox and metal dependence of the dimerization may have a physiological relevance. By taking together the structural results obtained for the nonactivated dimeric and the monomeric forms of *E. coli* Fur, new insights are gained into the molecular basis of Fur activation because of metal binding to the regulatory iron site. We propose that Fur activation implicates folding and unfolding of the untypical N-terminal helix observed in the metal-activated and in the monomeric forms of the Fur protein. Further experimental data are required to verify these hypotheses and to obtain a more profound comprehension of the function of this still very challenging protein.

Acknowledgments—We are indebted to Rutger Diederix for critical reading of the manuscript and Caroline Fauquant for help with the mutant construction.

REFERENCES

1. Hantke, K. (2001) *Curr. Opin. Microbiol.* **4,** 172–177
2. de Lorenzo, V., Wee, S., Herrero, M., and Neilands, J. B. (1987) *J. Bacteriol.* **169,** 2624–2630
3. Bagg, A., and Neilands, J. B. (1987) *Biochemistry* **26,** 5471–5477
4. Ochsner, U. A., Vasil, A. I., and Vasil, M. L. (1995) *J. Bacteriol.* **177,** 7194–7201
5. Adrait, A., Jacquamet, L., Le Pape, L., Gonzalez de Peredo, A., Aberdam, D., Hazemann, J. L., Latour, J. M., and Michaud-Soret, I. (1999) *Biochemistry* **38,** 6248–6260
6. Jacquamet, L., Dole, F., Jeandey, C., Oddou, J. L., Perret, E., Le Pape, L.,

Aberdam, D., Hazemann, J. L., Michaud-Soret, I., and Latour, J. M. (2000) *J. Am. Chem. Soc.* **122,** 394–395
7. Jacquamet, L., Aberdam, D., Adrait, A., Hazemann, J. L., Latour, J. M., and Michaud-Soret, I. (1998) *Biochemistry* **37,** 2564–2571
8. Althaus, E. W., Outten, C. E., Olson, K. E., Cao, H., and O'Halloran, T. V. (1999) *Biochemistry* **38,** 6559–6569
9. Gonzalez de Peredo, A., Saint-Pierre, C., Adrait, A., Jacquamet, L., Latour, J. M., Forest, E., and Michaud-Soret, I. (1999) *Biochemistry* **38,** 8582–8589
10. Coy, M., Doyle, C., Besser, J., and Neilands, J. B. (1994) *Biometals* **7,** 292–298
11. Pohl, E., Haller, J. C., Mijovilovich, A., Meyer-Klaucke, W., Garman, E., and Vasil, M. L. (2003) *Mol. Microbiol.* **47,** 903–915
12. Lewin, A. C., Doughty, P. A., Flegg, L., Moore, G. R., and Spiro, S. (2002) *Microbiology* **148,** 2449–2456
13. Michaud-Soret, I., Adrait, A., Jaquinod, M., Forest, E., Touati, D., and Latour, J. M. (1997) *FEBS Lett.* **413,** 473–476
14. D'Autréaux, B., Touati, D., Bersch, B., Latour, J. M., and Michaud-Soret, I. (2002) *Proc. Natl. Acad. Sci. U. S. A.* **99,** 16619–16624
15. Wee, S., Neilands, J. B., Bittner, M. L., Hemming, B. C., Haymore, B. L., and Seetharam, R. (1988) *Biometals* **1,** 62–68
16. Roth, M., Carpentier, P., Kaïkati, O., Joly, J., Charrault, P., Pirocchi, M., Kahn, R., Fanchon, E., Jacquamet, L., Borel, F., Bertoni, A., Israel-Gouy, P., and Ferrer, J. L. (2002) *Acta Crystallogr. Sect. D Biol. Crystallogr.* **58,** 805–814
17. Kabsch, W. (1993) *J. Appl. Crystallogr.* **26,** 795–800
18. Read, R. J. (2001) *Acta Crystallogr. Sect. D Biol. Crystallogr.* **57,** 1373–1382
19. Perrakis, A., Harkiolaki, M., Wilson, K. S., and Lamzin, V. S. (2001) *Acta Crystallogr. Sect. D Biol. Crystallogr.* **57,** 1445–1450
20. Emsley, P., and K. Cowtan, K. (2004) *Acta Crystallogr. Sect. D Biol. Crystallogr.* **60,** 2126–2132
21. Collaborative Computational Project (1994) *Acta Crystallogr. Sect. D Biol. Crystallogr.* **50,** 760–763
22. Jansson, M., Li, Y. C., Jendeberg, L., Anderson, S., Montelione, B. T., and Nilsson, B. (1996) *J. Biomol. NMR* **7,** 131–141
23. Tiss, A., Barre, O., Michaud-Soret, I., and Forest, E. (2005) *FEBS Lett.* **579,** 5454–5460
24. Morelle, N., Simorre, J. P., Caffrey, M., Meyer, T., Cusanovich, M., and Marion, D. (1995) *FEBS Lett.* **365,** 172–178
25. Brutscher, B., Cordier, F., Simorre, J. P., Caffrey, M., and Marion, D. (1995) *J. Biomol. NMR* **5,** 202–206
26. Szyperski, T., Braun, D., Fernandez, C., Bartels, C., and Wüthrich, K. (1995) *J. Magn. Reson.* **108,** 197–203
27. Wishart, D. S., and Sykes, B. D. (1994) *J. Biomol. NMR* **4,** 171–180
28. Farrow, N. A., Zhang, O., Forman-Kay, J. D., and Kay, L. E. (1994) *J. Biomol. NMR* **4,** 727–734
29. D'Autréaux, B. (2002) *Etudes Spectroscopiques de la Protéine FUR* (*Ferric Uptake Regulation*). *Interaction avec le Monxyde d'Axote.* Doctoral dissertation, Université J. Fourier, Grenoble, France
30. Gonzalez de Peredo, A., Saint-Pierre, C., Latour, J. M., Michaud-Soret, I., and Forest, E. (2001) *J. Mol. Biol.* **310,** 83–91
31. Saito, T., Duly, D., and Williams, R. P. J. (1991) *Eur. J. Biochem.* **197,** 39–42
32. Saito, T., and Williams, R. P. J. (1991) *Eur. J. Biochem.* **197,** 43–47
33. Saito, T., Wormald, M. R., and Williams, R. P. J. (1991) *Eur. J. Biochem.* **197,** 29–38
34. Laskowski, R. A., MacArthur, M. W., Moss, D. S., and Thornton, J. M. (1993) *J. Appl. Crystallogr.* **26,** 283–291
35. Barton, H. A., Johnson, Z., Cox, C. D., Vasil, A. I., and Vasil, M. L. (1996) *Mol. Microbiol.* **21,** 1001–1017
36. Coy, M., and Neilands, J. B. (1991) *Biochemistry* **30,** 8201–8210
37. Gonzalez de Peredo, A. (2000) *Etudes Structurale de la Protéine FUR* (*Ferric Uptake Regulation*). *d'Escherichia coli par Spectrométrie de Masse.* Doctoral dissertation, Université J. Fourier, Grenoble, France
38. Alekshun, M. N., Levy, S. B., Mealy, T. R., Seaton, B. A., and Head, J. F. (2001) *Nat. Struct. Biol.* **8,** 710–714
39. Garcia-Castellanos, R., Mallorqui-Fernandez, G., Marrero, A., Potempa, J., Coll, M., and Gomis-Ruth, F. X. (2004) *J. Biol. Chem.* **279,** 17888–17896
40. Friedman, Y. E., and O'Brian, M. R. (2004) *J. Biol. Chem.* **279,** 32100–32105
41. Servant, F., Bru, C., Carrere, S., Courcelle, E., Gouzy, J., Peyruc, D., and Kahn, D. (2002) *Brief Bioinform.* **3,** 246–251
42. Lee, J. W., and Helmann, J. D. (2006) *Nature* **440,** 363–367
43. Maret, W. (2004) *Biochemistry* **43,** 3301–3309
44. Guex, N., and Peitsch, M. (1997) *Electrophoresis* **18,** 2714–2723

Structural Changes of *Escherichia coli* Ferric Uptake Regulator during Metal-dependent Dimerization and Activation Explored by NMR and X-ray Crystallography

Ludovic Pecqueur, Benoît D'Autréaux, Jérome Dupuy, Yvain Nicolet, Lilian Jacquamet, Bernhard Brutscher, Isabelle Michaud-Soret and Beate Bersch

J. Biol. Chem. 2006, 281:21286-21295.
doi: 10.1074/jbc.M601278200 originally published online May 11, 2006

Figure S1: Electrostatic surfaces of *E. coli* Fur1-82 (left) and one *P. aeruginosa* Fur subunit (right). Both molecules are in the same orientation with the DNA-binding helix in the center as shown in the ribbon representation. Secondary structure elements of the N-terminal domain are indicated and helices are numbered I to IV, helix IV being the DNA-interaction helix. Note that for *P. aeruginosa* Fur, the whole subunit is shown, including the C-terminal domain.

Figure S1.